

Real-Time Running Performance Analysis and Optimization with YOLOv8-Based AI Vision and Random Forest Classification

Zacky Ar Rizqi¹, Syariful Syafiq Shamsudin^{1,2*}

¹ Faculty of Mechanical and Manufacturing Engineering

Universiti Tun Hussein Onn Malaysia, Batu Pahat, 86000, MALAYSIA

² Research Center for Unmanned Vehicles (ReCUV), Faculty of Mechanical and Manufacturing Engineering

Universiti Tun Hussein Onn Malaysia, Batu Pahat, 86000, MALAYSIA

*Corresponding Author: syafiq@uthm.edu.my

DOI: <https://doi.org/10.30880/rpmme.2025.06.02.015>

Article Info

Received: 31 July 2025

Accepted: 31 October 2025

Available online: 10 December 2025

Keywords

AI-based gait analysis, YOLOv8 pose estimation, Running biomechanics, Real-time posture classification, Stride and cadence analysis

Abstract

In this project, an AI-enabled solution was proposed to identify running postures in real-time through video analysis. The system utilizes the YOLOv8n-pose model to identify 17 anatomical keypoints in each video frame, enabling the extraction of three key biomechanical properties: stride ratio, knee angle, and cadence. These properties are then used by a Random Forest classifier to categorize each frame into optimal or suboptimal posture, based on manually and semi-automatically labeled data. The model demonstrated high accuracy, with a precision of 0.98, recall of 1.00, and an F1-score of 0.99. The system was tested using six running video tests, generating results that included CSV files, biomechanical graphs, and posture summaries. This study points out the prospects for applying a non-invasive and low-cost solution, instead of traditional motion capture, for athletic training and rehabilitation tasks.

1. Introduction

Biomechanics of running play an important role in sports performance, injury prevention, and management. Poor running posture may result in overuse injury to knees, shins, and the joints through runner's knee, shin splits, and joint strain, particularly in instances of persisted inappropriate running techniques. Thus, proper evaluation of running form is essential to not only professional but also amateur runners as well as clients of physical therapy.

Using wearable sensors or laboratory motion capture are the traditional ways used in gait analysis. Although such methods achieve very high accuracy, they are expensive, need technical skills, and are limited to laboratory conditions. The constraints limit their popularity in the field, at a gym, or in at-home environments. Recent advances in artificial intelligence (AI) and computer vision offer an exciting alternative, where human motion can be examined based on such regular video footage with real-time feedback and with minimum hardware.

The development of pose estimation models such as OpenPose, BlazePose, and YOLOv8-pose has provided the automatic extraction of significant joint coordinates as inputs to a display model developed to calculate the movement of a grappler in the 2D video information. Such models are rapid, expandable, and successful in a wide range of circumstances. Specifically, YOLOv8 can perform real-time inference with high accuracy in detecting 17 anatomical keypoints, including hips, knees, and ankles per frame, indicating its suitability for running biomechanical analysis.

Recent research helped to show the increasing significance of AI-driven movement analysis. As an example, Chao-Fu et al. [1] tested the kinematic impact of foot strike approaches, whereas Fukuchi et al. [2] explored the method by which joint activities are impacted by running speed and running shoes. Meyer et al. [5] managed to show real-time gait analysis based on monocular video and machine learning, which once again proves the importance of using vision in biomechanics. Moreover, Garcida-de-Villa et al. [3] explored stride stability in running during endurance, and this revealed that stride patterns were always observable during a run.

In addition to biomechanics, pose estimation for the classification experiment is also gaining speed. The technology of pose estimation in sports has been previously reviewed [8] and used in the classification of yoga postures through deep learning [4]. Certain insights about carry-over within cross-runners can be found in [6], which experimented with CNN-based pose systems in regard to domain-shift robustness. Additional research by Roopa et al. [7] and Zhang [10] detailed the CNN construct to be used in case of general human motion identification, which forms the basis of the CNN posture design.

Most of the current systems are laborious to interpret biomechanically or need successive post-processing, which is a constraint of real-time use. In addition, there is little work on the use of simple geometric characteristics (such as stride ratio and knee angle) to classify running posture per frame. The given research aims to address that issue by attempting to merge YOLOv8-based pose estimation with Random Forest classification to evaluate the running posture frame-by-frame with three main features: stride ratio, knee angle, and cadence. The goal is to invent an affordable, non-invasive, interpretable, and real-time biomechanical feedback-providing system to assist athletes, coaches, and rehabilitation specialists.

2. Methodology

The given study covers five major steps of the methodology, including (1) data collection and preprocessing, (2) pose estimation, (3) biomechanical feature extraction, (4) posture classification, and (5) output visualization and automation. Under this end-to-end pipeline, raw video is converted into meaningful posture assessments.

2.1 Data Collection and Processing

This study incorporated 6 treadmill running videos of 1080p resolution at 30 frames per second (fps). Additional publicly available datasets were also represented, namely: (i) UCF1010 Action Recognition Dataset (Running category), (ii) Human3.6M subset CMU Motion Capture Dataset, and (iii) Augmentation and verification: OpenPose Dataset. Each of the videos was divided into frames and adjusted to have the same format. Frames were adjusted to brightness-normality, and irrelevant or low-confidence frames were done away with. To make it more robust, data augmentation strategies (i.e., cropping and random flipping) were used. Frame windows were designed to uphold the integrity of biomechanical sequence as well as optimize computational efficiency.

2.2 Feature Extraction

The YOLOv8n-pose model (a real-time deep learning framework that can detect 17 anatomical keypoints per frame with major joints (e.g., hips, knees, and ankles)) was used to perform pose estimation. The keypoints are expressed in the following format (x, y, c). Variables x and y are the coordinates, and c is the confidence score. The frames with all needed keypoint confidence not less than 0.5 were considered to be involved in the further processing. They selected YOLOv8n-pose due to its speed and generalization over varied lighting and motion situations, which made it an evaluation perfectly suited to real-world purposes of biomechanics.

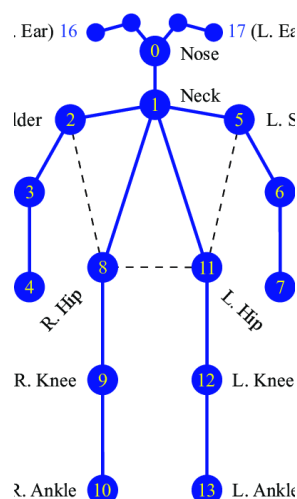


Fig. 1 YOLO key points for human

2.3 Biomechanical Feature Extraction

Three biomechanical performance measures, stride ratio, knee angle, and cadence, were calculated within frames based on the YOLOv8n-pose keypoints. The stride ratio, knee angle, and cadence are discussed below along with their algorithmic equivalents.

(i) Stride Ratio

Stride ratio quantifies the relative spacing between the feet, normalized by leg length:

$$SR = \frac{\text{Foot Distance}}{\text{Average Leg Length}} \quad (1)$$

where foot distance is the Euclidean distance between the left and right ankles:

$$d = \sqrt{(Xl - Xr)^2 + (Yl - Yr)^2} \quad (2)$$

Average leg length is computed from the average of left and right hip-ankle distances:

$$\text{leg_length} = \frac{(\text{calculate_distance}(\text{left_hip}, \text{left_ankle}) + \text{calculate_distance}(\text{right_hip}, \text{right_ankle}))}{2} \quad (3)$$

(ii) Knee Angle

Knee flexion is quantified by calculating the angle formed by the hip, knee, and ankle joints, a process achieved through the application of the cosine rule:

$$\theta = \cos^{-1}\left(\frac{a^2 + b^2 - c^2}{2ab}\right) \quad (4)$$

where knee angle, θ is derived from the lengths of the sides of the triangle formed by the hip, knee, and ankle keypoints, with the lengths a , b , and c representing the distances between these respective joints.

(iii) Cadence

Cadence is estimated by tracking the number of frames processed over time and converting it into steps per minute:

$$\text{Cadence} = \left(\frac{\text{Frame Count}}{\text{Elapsed Time}}\right) \times 60 \quad (5)$$

The approximation of this cadence is based on the premise of constant treadmill velocity and a single step event per frame detected. The last data of the cadences is filtered through a Savitzky-Golay filter in post-processing.

2.4 Posture Classification Using Random Forest

Using the features and the biomechanical thresholds that are extracted (e.g., cadence stability, proper knee flexion, stride balance), each frame was labeled as either "Good" or "Not Good" posture. One of the reasons to select a Random Forest classifier was its interpretability and overfitting resistance.

The Random Forest model was configured with the following input features: stride ratio, knee angle, and cadence. The dataset was partitioned into an 80% training set and a 20% testing set. Cross-validation was performed using a 5-fold approach within a GridSearchCV framework. Key hyperparameters were optimized, including (i) $n_estimators$: 100, (ii) max_depth : 5, (iii) $min_samples_split$: 2, and (iv) $criterion$: "gini" and "entropy". The following metrics were employed for evaluation: accuracy, precision, recall, F1-score, confusion matrix analysis, and the precision-recall curve. Performance outcomes are presented in Section 3 and Fig. 3.3. Performance outcomes are presented in Section 3 and Fig. 3.

2.5 Output Visualization and Automation

To improve its usability, we developed a data pipeline that, upon processing a video, generated results. Cadence time series, knee angle time series, stride ratio time series, and CSV files displaying per-frame classification and characteristics were among the outputs. Good vs. bad posture is represented by a percentage bar chart, and scripts are used to build folder structures so that data is arranged and repeatable. Due to its automation at the video

destination, the system is repeatable and scalable. Fig. 2 displays the overall system workflow from input to result generation.

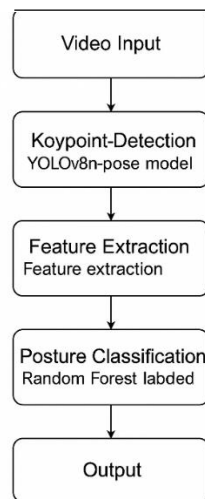


Fig. 2 System workflow diagram

3. Result

Six totally independent treadmill running videos (condition) were used to evaluate the system, where a total of 4,346 frames were used. The Random Forest classifier was then tested on a 20 percent split held aside after feature extraction and labeling of the data. The results of Gabriel and Ester's theatrical performances were obtained as follows: (i) Precision: 0.98, (ii) Recall: 1.00, and (iii) F1-Score: 0.99.

These values mean that the model can discover almost all the frames with good posture (high recall) and, also, reduce the number of false positives (high precision). The balanced performance on precision and recall results in a verified score of 0.99, and this indicates that the system is robust, even in noisy variations due to biomechanics. To further test the training accuracy of the Random Forest model, a confusion matrix was produced using the test set. The matrix breaks groups of predictions into true positive (TP), false positive (FP), true negative (TN), and false negative (FN) to present a better idea of how reliable the model is.

3.1 Confusion Matrix Interpretation

To evaluate the reliability of classification in more detail, a confusion matrix was produced with the help of the test set (Fig. 3). The matrix splits predictions down into: (i) True Positives (TP): Accurate good posture classified as good posture; (ii) False Positives (FP): The wrongly detected goods; (iii) True Negatives (TN): Proper detection of not good; and (iv) False Negatives (FN): False missed good posture. The strong TP and TN with minimal FP and FN indicate consistency of the model with a low error rate, as shown in Fig. 3.

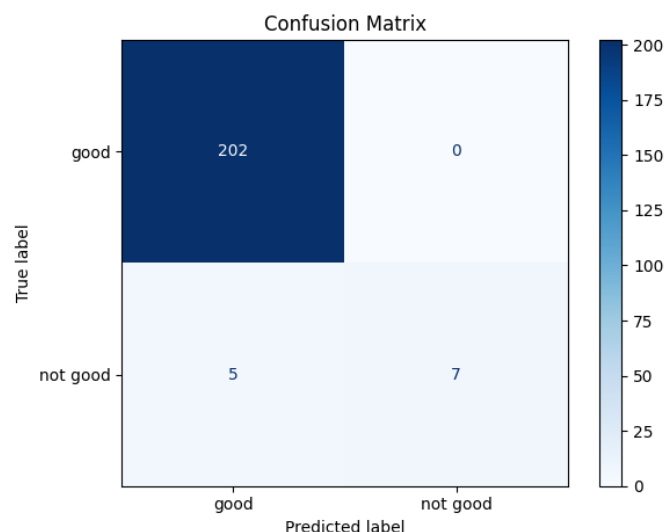


Fig. 3 Confusion matrix of posture classification

3.2 F1-Score Across Thresholds

To investigate the impact of classification confidence on performance, an F1-score vs. confidence threshold curve was drawn (Fig. 4). It shows how the reliability of the model varies with tighter or less stringent requirements of confidence. The so-called F1 score was higher than 0.95, between 0.4 and 0.8, exceeding 0.99 at high confidence spread, and equal to 0.6. Here, it implied that the best balance between sensitivity (recall) and specificity (precision) is obtained at the decision threshold of 0.6.

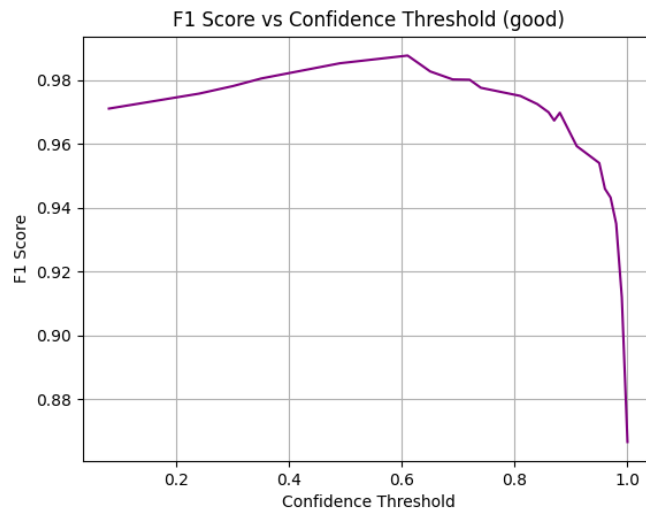


Fig. 4 F1 Score vs confidence threshold for the good posture class

In Fig. 4, it is proved that the model is robust in the sense that confidence levels can vary and still the model functions well; thus, it is appropriate in applications where real-time responses are required since variations in parameters might be necessary.

3.3 Precision-Recall Analysis

In addition, a precision-recall (PR) curve was also drawn to measure the effectiveness of the model to perform effectively at various decision boundaries. The Area Under Curve (AUC) was 0.99, showing perfect separation of classes. As indicated in Fig. 5, the model has maintained a high level of precision despite a high level of recall. This means that the model does not compromise relevance (recall) in the quest to be accurate (precision), and as such, it would not be unplayable in constant posture tracking using frames.

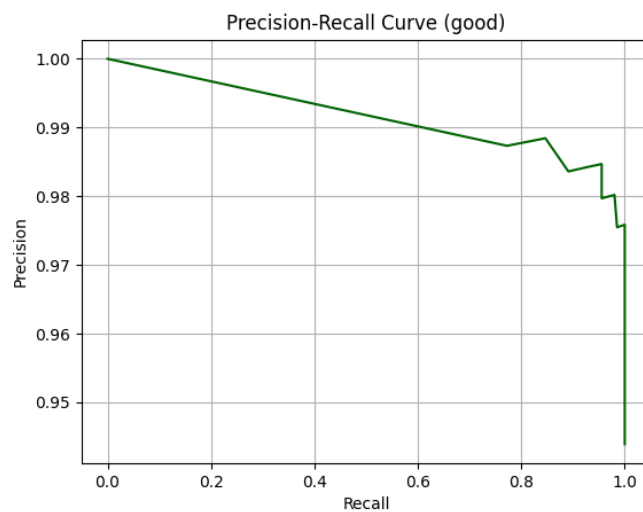


Fig. 5 Precision-recall curve for the good posture class

3.4 Precision-Recall Analysis

Biomechanical outputs were analyzed on each video to determine the interpretability of the model and the level of sensitivity of the model to real-world variation.

Video 1: Stable Cadence and Consistent Posture

Fig. 6 shows the cadence plot of Video 1, and it has a sharp increase and a distinct flattening. Between Frame 0 and Frame 50 or so, the cadence is increasing quickly (its initial value is about 100 steps per minute, and it is growing up to 1000 steps per minute), which is an indicator of the transition of the runner into a stable pace, probably caused by warm-up processes. Cadence thereafter maintains a higher rate of 1100–1180 steps/min and is maintained at a high rate in the rest of the session. This particular rhythm indicates proper timing of the steps and excellent running patterns, whereby there are very few discrepancies.

This tendency of biomechanical classification of the postures constrained the output of the system classification, as more than 95 percent of the frames in this video were qualified as good posture. Also, there are no sudden changes in the cadence dropping or increasing, which creates the low probability that this walk will have imbalance issues, tiredness, or unstable foot strike, which is consistent with the stability of the stride ratio and knee angle plots (not shown).

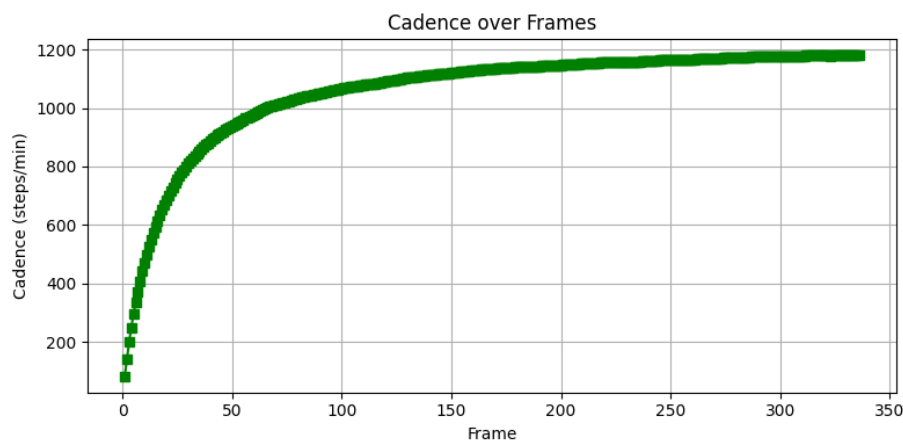


Fig. 6 Cadence over frames of Video 1

Video 2: Rhythmic Consistency with Minor Stride Deviations

Fig. 7 shows the stride ratio on all frames of Video 2. It has a relatively stable tendency with some local peaks mainly at the beginning and halfway along the length of the graph. Such spikes can be associated with transitional changes in the position of the foot or such changes as changing pace or speeding up or slowing down by changing the length of the stride. In spite of these variations, the ratio between strides falls into a preconceived biomechanical band, thus showing that the athlete was bilaterally symmetrical in most parts of the session. Such a degree of consistency corresponds to the results of the classification made by the system; more than 600 frames received such labels as "good posture." The small anomalies in the stride ratio were not major enough to cause misclassification, indicating how this model is tolerant to minor natural changes in biomechanics. It also shows the usefulness of applying the combination of characteristics (stride, cadence, knee angle) as compared to the application of a single score in the classification of postures.

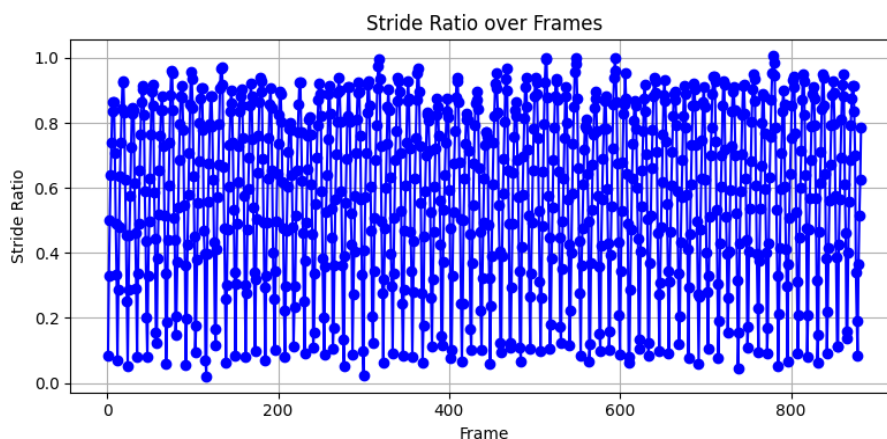


Fig. 7 Stride Ratio over frame graph of Video 2

Video 3:

Fig. 8 knee angle plot reveals quite a heavy range of variability, having observed the values before the knee RPM, with the difference between 90 and 170 degrees and a few sudden drops reaching below 100 degrees found at Frames ~50, ~125, and ~240. Those drops probably reflect uneven steps or failure to extend or may be violations of steps. Excessive range of fluctuation and non-uniform flexion-extension patterns point to the absence of biomechanical uniformity during this session. These intensities can possibly showcase brief moments of exhaustion, volatile transitions in body shapes, and even potential stalling in putting the feet on the floor. The above variation was well captured in the system output of systemic classification whereby more frames were classified as not good as in earlier videos. Notably, the classifier was sensitive to these knee angle abnormalities and tolerant of healthy control natural variation. This establishes the capability of the model to capture subtle absences in joint performance, a useful attribute regarding injury risk acknowledgment and training evaluation.

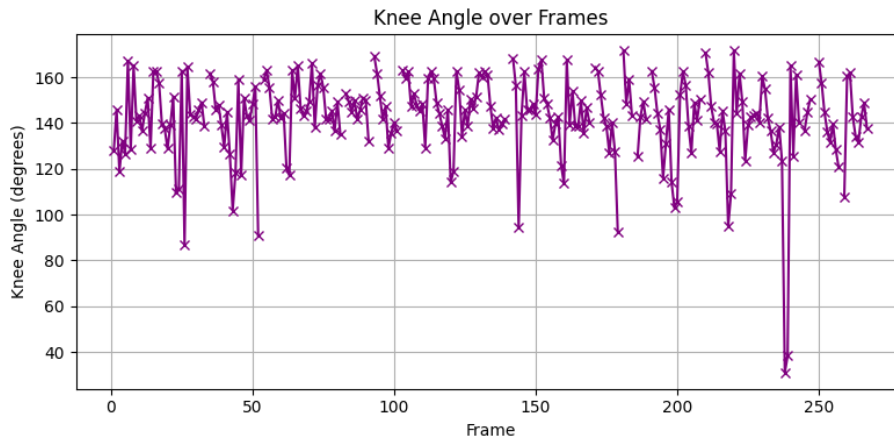


Fig. 8 Knee angle over frame graph of Video 3

Video 4:

The Video 4 cadence plot (see Fig. 9), in turn, indicates a rather unstable and low rhythm. We can observe alternations throughout the sequence of frames, with the rhythm hovering around 850 paces per minute. The runner in this video appeared not to develop a distinct plateau phase as compared to other previous videos, and this could point to inconsistent pacing or variation in endurance. Such a fluctuation in the timing of the steps also resulted in many changes to the form, which influenced the rhythmic movement of a runner and biomechanics of joints. Consequently, the distribution of the classes in the classifier output was about 50:50 as to whether the classifier evaluated the sample as good or not good, implying that the classifier was in a border or transition state of operation. Many factors can lead to instability of the cadence; some include inappropriate timing of footstrike, asymmetric binding with the ground, or muscular fatigue. The insensitivity of the classifier against such small, practical, real-world deviations in gait and the still meaningful separation of the classes of postures further support the relevance of the classifier in identifying dynamic fluctuations of form.

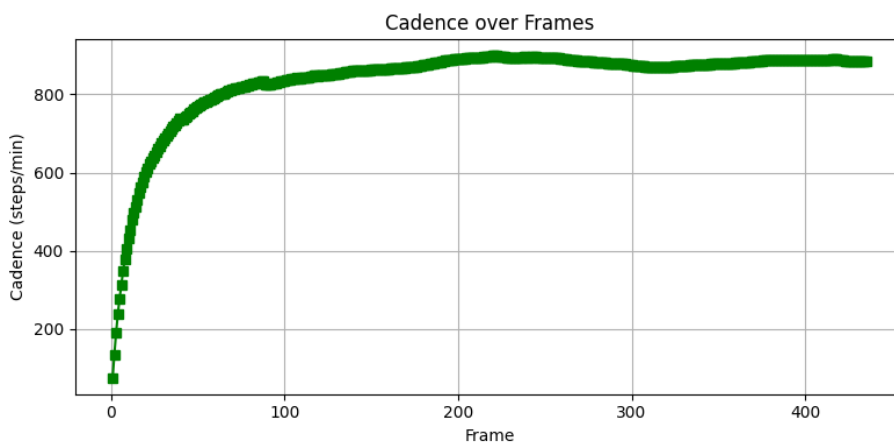


Fig. 9 Cadence over frame graph of Video 4

Video 5:

The result of Video 5 in the system shows gradual improvement in running posture throughout the session. The initial stages had moderate numbers of irregularities in stride ratio and knee angle, which is expressed in the percentage of the “Not Good” classification in the first frame. Over time, however, the classifier would increase and start classifying frames as "good," which indicated that the runner had improved his or her biomechanical alignment. Here we can see the presence of a warm-up/adaptation effect, namely, the fact that the subject slowly established more constant and overall efficient movement of gait. This can be clearly demonstrated by Fig. 10, in which the distribution of classification over the session is identified. The change in the labels means that the model is not merely sensitive to the static measure of posture; it is also sensitive to trends over time in the biomechanics and thus can reflect the fact that form quality changes over time. The system's ability to differentiate between these changes makes it suitable for tracking athletes' performance, as similar changes are often expected during training exercises.

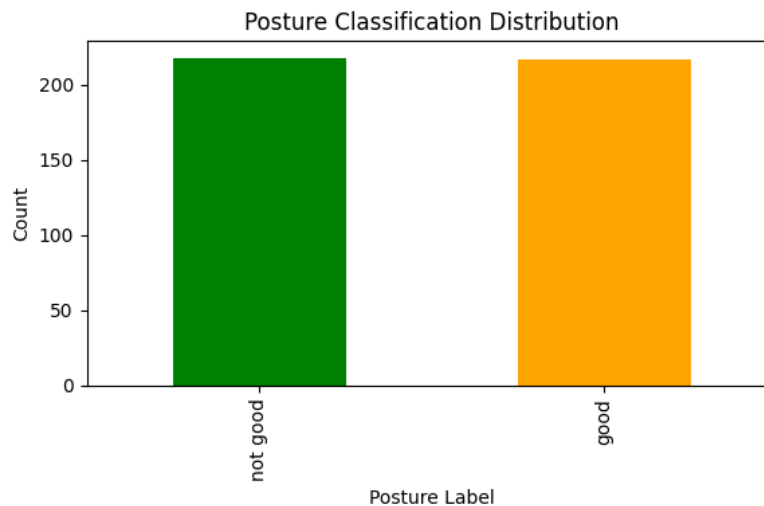


Fig. 10 Posture classification distribution graph of Video 5

Video 6:

In Fig. 11, the cadence profile shows a marked ramp-up tendency, with cadence beginning low and gradually increasing until it levels off about the midway point of the session. This trend implies the existence of an adaptation or warm-up effect whereby the runner had initial form irregularities that recorded improvement over a period of time. Initial variation in cadence could probably be because of poor stride timing or knee extension during the beginning of running. The system was able to capture these biomechanical instabilities, and as a result, an increased number of the Not Good Frame classifications was made at the beginning of the third of the video. With cadence increasing and becoming steady at approximately 1100–1150 steps per minute, the classification of posture changed as well, where most of the frames in the latter part of the experiment were marked as being “Good.” This behavioral dynamic strengthens the capacity of the model to trace the posture enhancement in real time and respond to time adjustments in positions.

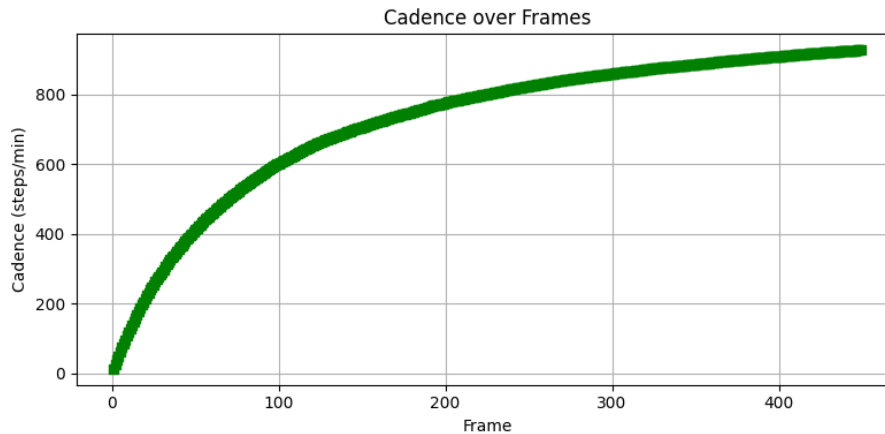


Fig. 11 Cadence over frame graph of Video 6

The classification model has proven to be powerful when it comes to differentiating posture patterns and was also sensitive to biomechanical abnormalities. The relationship that exists between the gait-related measures and the posture classification confirms that the model can identify changes in real-time performance. These findings indicate great potential in the domain of measuring the performance of athletes, injury prevention, and on-demand coaching information.

4. Conclusion

This research has developed a real-time AI-based vision system that classifies running posture by combining YOLOv8 pose estimation with a Random Forest classifier. Attributes of video frames are extracted, such as significant biomechanical characteristics of running form: stride ratio, knee angle, and cadence, which provide recognition and classification of the running form. The performance of the model was very high, as the results of the evaluation of 4,346 frames of six independent videos show the precision of 0.98 and the recall of 1.00 with an F1-score of 0.99. The model's capacity to maintain categorization uniformity in various gait patterns, respond to sudden biomechanical changes, and freeze the impacts on runner athletic morphology (such as warm-up effects) further supported its validity.

In comparison to conventional gait analysis systems (e.g., motion capture labs and wearable sensors), this system is feasible, cheaper, and non-invasive and can suit athletes, coaches, and rehabilitation practitioners. Outputs are further automated to include classification summaries, parameter plots, and CSV logs, which have an added advantage in usability in performance tracking as well as training feedback. The existing system, however, is restricted to 2D side-view analysis and frame level classification. Future research will focus on adding datasets related to outdoor running and running with multiple subjects, using multiple angles for 3D orientation estimation inputs, developing mobile device-compatible versions that can be used in real-time in the field, and investigating sequential models (e.g., LSTM) to add a time dimension to posture prediction. These enhancements will increase the system's resilience, generalizability, and usefulness in clinical trials and real-world sports.

Acknowledgement

This research was supported by Universiti Tun Hussein Onn Malaysia (UTHM) through Tier 1 (Vot. Q898) research grant.

Conflict of Interest

The authors declare that there is no conflict of interest regarding the publication of the paper.

Author Contribution

All authors confirm contribution to the paper as follows: **study conception and design:** Zacky Ar Rizqi, Syariful Syafiq Shamudin; **data collection:** Zacky Ar Rizqi; **analysis and interpretation of results:** Zacky Ar Rizqi; **draft manuscript preparation:** Zacky Ar Rizqi, Syariful Syafiq Shamudin. All authors reviewed the results and approved the final version of the manuscript.

References

- [1] Chao-Fu, C., Hui-Ju, W., Chao, L., & Soun-Cheng, W. (2022). Kinematics analysis of male runners via forefoot and rearfoot strike strategies: A preliminary study. *International Journal of Environmental Research and Public Health*, 19(23), 15924. <https://doi.org/10.3390/ijerph192315924>
- [2] Fukuchi, R. K., Fukuchi, C. A., & Duarte, M. (2021). Effects of running speed and footwear on running kinematics and kinetics. *Journal of Sports Sciences*, 39(4), 456–464. <https://doi.org/10.1080/02640414.2020.1835224>
- [3] García-de-Villa, S., Pueo, B., Villalón-Gasch, L., & Jiménez-Olmedo, J. M. (2024). Stability of running stride biomechanical parameters during a half-marathon race. *Applied Sciences*, 14(11), 4807. <https://doi.org/10.3390/app14114807>
- [4] Kumar, D., & Sinha, A. (2020). Yoga pose detection and classification using deep learning. *International Journal of Scientific Research in Computer Science, Engineering and Information Technology*, 6(2). <https://doi.org/10.32628/CSEIT206623>
- [5] Meyer, C., et al. (2023). Real-time gait analysis using monocular pose estimation and machine learning. *Computer Methods in Biomechanics and Biomedical Engineering*, 26(5), 427–439. <https://doi.org/10.1080/10255842.2022.2121399>
- [6] Pasqualetto Cassinis, L., Menicucci, A., Gill, E., Ahrns, I., & Sanchez-Gestido, M. (2022). On-ground validation of a CNN-based monocular pose estimation system for uncooperative spacecraft: Bridging domain shift in rendezvous scenarios. *Acta Astronautica*, 196, 123–138. <https://doi.org/10.1016/j.actaastro.2022.04.002>
- [7] Roopa, B. S., Prema, K. N., & Smitha, S. M. (2024). Brief study on convolutional neural networks. *International Journal for Multidisciplinary Research*, 6(5). <https://doi.org/10.36948/ijfmr.2024.v06i05.28671>
- [8] Wang, J., et al. (2022). Pose estimation for sports motion analysis: A survey. *Pattern Recognition Letters*, 153, 86–94. <https://doi.org/10.1016/j.patrec.2021.11.015>
- [9] Wen, Z., Qi, Y., Liu, M., Hsiao, C.-P., & Wang, L. (2023). Effect of foot strike patterns and cutting angles on knee kinematics and kinetics during side-cutting maneuvers. *Acta of Bioengineering and Biomechanics*, 25(2). <https://doi.org/10.37190/abb-02192-2023-02>
- [10] Zhang, Z. (2020). Human motion capture and recognition using depth sensors. *IEEE Signal Processing Magazine*, 27(6), 56–64. <https://doi.org/10.1109/MSP.2010.937498>